Food Chemistry: X 20 (2023) 100946

Contents lists available at ScienceDirect

Food Chemistry: X

journal homepage: www.sciencedirect.com/journal/food-chemistry-x

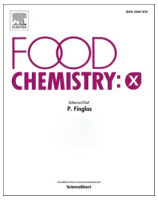

# Effects of eugenol on the structure and gelling properties of myofibrillar proteins under hydroxyl radical-induced oxidative stress

Deyin Pan [a,b,1], Jinming Ma [a,b,1], Jingjing Diao [a,b], Jiaqi Li [a,b], Hongsheng Chen [a,b,*]

[a] College of Food Science, Heilongjiang Bayi Agricultural University, Daqing, Heilongjiang 163319, China
[b] Heilongjiang Food and Biotechnology Innovation and Research Center (International Cooperation), Daqing, HeilongJiang 163319, China

ARTICLE INFO

*Keywords:*
Eugenol
Protein oxidation
Myofibrillar protein
Rheology
Water distribution

ABSTRACT

The effects of eugenol (EG; 0, 5, 20, and 50 mg/g protein) on the structure and gel properties of pork myofibrillar protein (MPs) under a hydroxyl radical-generating system were explored in this study. The results revealed that the addition of a high concentration of EG (50 mg/g protein) markedly reduced the carbonyl content and enhanced the fluorescence intensity, surface hydrophobicity, and protected the secondary structure of MPs, compared to oxidized MPs. In addition, the high concentration group noticeably increased the storage modulus ($G'$), gel strength, and water-holding capacity (WHC), and significantly hindered the oxidation-induced transformation of immobilized water of the MPs gel to free water and basically favored the formation of a finer and more homogeneous three-dimensional network structure, This work verified that the adding of EG could effectively improve the gel quality of oxidized MPs and more successfully delay oxidation-induced damage to muscle protein structure.

## 1. Introduction

Muscle food plays an important role in human nutrition due to its rich content of high-quality proteins, mainly myofibrillar proteins (MPs), sarcoplasmic proteins, and matrix proteins. The MPs comprise approximately 55–60 % of total muscle protein and are the primary structural component of muscle (Chen, Chen, Cheng, & Liang, 2022). The emulsification, gelation, and water retention properties of MPs are some of the most important functional characteristics in processed meat products. However, the gel-forming ability of MPs is particularly susceptible to physical and chemical factors during the processing and storage of raw meat. Proteins in meat are extremely sensitive to oxidative damage owing to the high amounts of endogenous pro-oxidant transition metals (e.g. iron and copper), haemoglobin and polyunsaturated fatty acids in muscle tissue, as well as molecular oxygen that enters the meat during processing (Cao, Ma, Huang, & Xiong, 2020). So an oxidative environment is the primary factor that leads to changes in protein conformation and aggregation, which also affects protein functions, such as water-holding capacity (WHC), emulsification properties, and gelling properties (Zheng et al., 2021).

Scientists are working tirelessly on a variety of dietary (feed-based) and technological (formulation/packaging) approaches to reduce protein oxidation in order to improve the functional properties of proteins in meat products (Estévez & Heinonen, 2010). In this regard, synthetic antioxidants have long been used as food additives to reduce protein oxidation and delay the deterioration of the quality of meat products. However, these added substances tend to have secondary effects on organoleptic and culinary characteristics and can sometimes have long-term adverse effects on consumers' health (Torrecilhas et al., 2021). Such health-related concerns and the environmental issues regarding synthetic chemicals used as preservatives have driven the popularity of the clean-label product movement currently sweeping the food industry.

As natural alternatives to synthetic antioxidants, the ability of spices and herbs to inhibit protein oxidation in various food systems has been reported extensively. Plant extracts rich in phenolic acids are commonly added to emulsion-type meat products for flavor modification and oxidative stability (Jiang & Xiong, 2016). Taguri, Tanaka, and Kouno (2004) showed that polyphenols from various foods and herbs are beneficial to human health, and extracts of some polyphenol-rich plants have been applied to functional foods or capsules. In proteinaceous foods, plant phenolics can interact with proteins through both non-covalent and covalent bonds to modify protein functional groups,

* Corresponding author at: College of Food Science, Heilongjiang Bayi Agricultural University, Daqing, Heilongjiang 163319, China.
*E-mail address:* hsch0608@163.com (H. Chen).
[1] The authors contributed equally to this work.

https://doi.org/10.1016/j.fochx.2023.100946
Received 30 July 2023; Received in revised form 5 October 2023; Accepted 13 October 2023
Available online 29 October 2023

structure stability, aggregation, and solubility, leading to functionality changes, especially for gelation, which is the most important texture-forming property in processed muscle foods (Cao & Xiong, 2015).

Eugenol (EG) is one of the most active components in clove and has exceptional antioxidant properties (Chen et al., 2016). This naturally active substance has also been highlighted for its antibacterial, antiseptic, analgesic, and anesthetic properties (Marchese et al., 2017). EG is reported to donate electrons to free radicals, transforming them into more-stable, less reactive species and terminating the free radical chain reaction (Tan, Ye, Liu, & He, 2010). El-Maati et al. (2016) reported that the antioxidant activity of EG was comparable to vitamin E. In the meat industry, EG is commonly added to feed to reduce fat oxidation and pigment degradation and to enhance the antioxidant activity in meat. In this context, adding essential oils containing EG (4 g/day) to the rations of Nellore heifers was found to significantly increase average daily weight gain and dry matter intake (Souza et al., 2019). Lin et al. (2023) prepared a highly encapsulated and stable gelatin active packaging film loaded with EG nanoparticles as an active component and then showed that the developed film could be applied as active packaging to extend the shelf life of chicken breast. In another study of note, bioactive antibacterial EG-loaded gelatin nanofibers fabricated specifically for beef samples maintained their textural properties (hardness, gumminess, and chewiness) and sensory properties during the 9-day storage period (Yilmaz, Hassanein, Alkabaa, & Ceylan, 2022). Furthermore, EG is a promising antimicrobial agent to control foodborne outbreaks by reducing the campylobacter load in the production process of poultry meat (Gürbüz & Korkmaz, 2022). It has also been shown to impede the biofilm formation of *Salmonella enterica ser. Typhimurium* and *Listeria monocytogenes* (Purkait, Bhattacharya, Bag, & Chattopadhyay, 2020), two common foodborne pathogens found in the meat production chain. However, in the existing literature, few studies have explored the impact of EG on the oxidative stability and gelation behavior of MPs.

As the hydroxyl radical-generating system is widely employed in meat processing and is considered the most potent oxidizing radical among reactive oxygen radicals. Therefore, the aim of this study was to add EG as an antioxidant into an MPs oxidation system, which could be applied in comminuted meat batters not only to produce an excellent gelation performance but also to provide an effective antioxidant effect on meat products. Physicochemical, structural, and rheologic analyses were carried out to illustrate the underlying interaction mechanisms. Gaining insights into these underlying mechanisms can facilitate the development of formulae for restructuring meat products with healthier and desirable characteristics.

## 2. Materials and methods

### 2.1. Materials

Beidahuang Meat Processing Co., Ltd is a standard farm of Harbin in China, and the conditions of rearing are standardized. The pigs were electro-stunned before slaughter, after slaughtered by standard commercial procedures, the carcasses were aged at 4 °C for 24 h to dissipate rigor mortis. Fifteen entire carcases were randomly selected from a large population. The longissimus lumborum muscles (core temperature of 4 °C, pH 5.8–6.2) of pork were obtained from Beidahuang Meat Industry Co. Ltd. (Daqing, China) and then cut into 90 ~ 110 g pieces, for a total of 150 pieces, then were vacuum-packaged and stored in a – 30 °C freezer until use in less than 2 months. Followed by MPs extraction at 4 °C within 36 h after slaughter using the method described by Park, Xiong, and Alderton (2007). Trolox (≥98 % purity) was purchased from Solarbio Chemical Co. (Beijing, China). EG (≥99 % purity) was obtained from Shanghai Macklin Biochemical Co. Ltd. (Shanghai, China). All other analytical grade chemicals were purchased from Aladdin Chemical Co. Ltd. (Shanghai, China) and Sigma Chemical Co. Ltd. (St. Louis, MO, USA).

### 2.2. MPs oxidation and treatment with EG

The freshly extracted MPs were diluted to concentrations of 20 and 30 mg/mL. Then, 60 mmol/L EG solution was mixed with the MPs solution in different proportions to obtain a gradient concentration series of EG − MP suspensions. The samples were oxidized at 4 °C for 12 h using a hydroxyl radical (•OH)-generating mixture (10 μmol/L $FeCl_3$, μmol/L ascorbic acid, and 10 mmol/L $H_2O_2$) (Geng et al., 2018). The final EG concentrations were 5, 20, and 50 mg/g protein; we designated these concentrations as low, medium, and high ($EG_L$, $EG_M$, and $EG_H$, respectively), and the corresponding oxidized EG − MP suspensions as O + $EG_L$, O + $EG_M$, and O + $EG_H$, respectively. The oxidation reaction was terminated by the addition of Trolox (1 mmol/L, final concentration). Protein solutions exposed to oxidation treatment without EG and those without EG and the oxidation treatment but containing Trolox served as the oxidized (O) and non-oxidized (No-O) controls. The concentrations for EG were selected based on a relevant previous study (Chen et al., 2023) and our preliminary trials.

### 2.3. Determination of chemical changes of MPs

#### 2.3.1. Carbonyl content

Carbonyl groups of the MPs were determined using the 2,4-dinitrophenylhydrazine (DNPH) colorimetric method described by Rajkovic, Tomasevic, De Meulenaer, and Devlieghere (2017). The carbonyl content was calculated by spectrophotometric measurement of the absorbance at 370 nm using a molar extinction coefficient of 22,000 $M^{-1}$ $cm^{-1}$, and the result was expressed as nmol carbonyl/mg MP.

#### 2.3.2. Total sulfhydryl content

According to the method of Cao & Xiong (2015), the total sulfhydryl content of MPs was determined using Ellman's reagent [5,5′-dithiobis(2-nitrobenzoic acid), DTNB] reagent by ultraviolet spectrophotometric measurement of the absorbance value at 412 nm, and the result was expressed as nmol sulfhydryl/mg MP.

#### 2.3.3. Free amines

The free amine content was determined at 420 nm using the 2,4,6-trinitrobenzenesulfonic acid (TNBS) method described by Cheng, Zhu, & Liu (2020). The amount of free amines in the MP samples was calculated using a standard curve generated with L-leucine.

### 2.4. Determination of structural changes in MPs

#### 2.4.1. Secondary structure

Full-band Fourier-transform infrared (FTIR) spectra were recorded using a TENSOR II infrared spectrometer (Bruker Co. Ltd., Tianjin, China) to analyze the secondary structures in the MP samples (dry form). The protein samples with and without EG were mixed with potassium bromide, ground, and pressed prior to scanning from 400 to 4000 $cm^{-1}$ using the FTIR instrument. All data were processed by baseline correction, automatic smoothing, deconvolution, second-order derivation, and fitting using OMNIC software and Peakfit 4.12 software to analyze the protein amide I band changes.

#### 2.4.2. Tertiary structure

According to the method of Gan, Li, Wang, et al. (2019). A fluorescence spectrometer (970 CRT, Jingke Co. Ltd., Shanghai, China) was operated at an excitation wavelength of 282 nm and an emission spectral range from 290 to 420 nm. Both the excitation and emission slits were set at 5.0 nm. The fluorescence of the diluted EG − MP mixed suspension (final protein concentration of 0.25 mg/mL) was measured at room temperature.

#### 2.4.3. Surface hydrophobicity ($H_o$)

The $H_o$ of MPs was determined using the hydrophobic chromophore

bromophenol blue (BPB) according to the method of Benjakul, Visessanguan, Ishizaki, and Tanaka (2001). The absorbance values of the blank solution ($A_{blank}$) and the mixed supernatant of EG − MP (diluted 10 times; $A_{sample}$) were measured at 595 nm. The $H_o$ was calculated by the following equation:

$$\text{Bound BPB} = 100\,\mu g \times \frac{A_{blank} - A_{sample}}{A_{blank}}$$

### 2.5. Protein cross-linking

The influence of EG addition on protein cross-linking during the reaction process was determined using sodium dodecyl sulfate–polyacrylamide gel electrophoresis (SDS-PAGE) according to Chen et al. (2016). with a 3 % polyacrylamide stacking gel and a 12 % resolving gel. Each diluted MP sample (2 mg/mL) was mixed with an equal volume of SDS-PAGE sample buffer with or without 5 % β-mercaptoethanol (βME) and boiled for 3 min.

### 2.6. Gel properties

#### 2.6.1. Dynamic rheology

Using a DHR-1 hybrid rheometer (TA Instruments, Inc., New Castle, DE, USA) in oscillating mode, the MPs suspension (1.5 mL with a final protein concentration of 30 mg/mL) was placed between two parallel plates with a 1 mm gap and equilibrated at 20 °C for 2 min after adding glycerol around the sample. The sample was heated from 20 to 72 °C, and the dynamic rheological properties of the MP samples during gelation were determined by measuring the storage modulus ($G'$), following the method described by Huang et al. (2022).

#### 2.6.2. Gel strength

A glass vial (inner diameter of 16.5 mm and length of 50 mm) containing a threaded plastic cap was used to weigh 8 g of the EG − MP suspension, which had a final protein concentration of 30 mg/mL. The suspension was heated from 20 to 75 °C to prepare a heat-induced MP gels, and then the vials were immersed in ice water for 30 min before being placed in a refrigerator at 4 °C overnight. Gel strength was measured using a P/0.5 probe on a TA.XTplusC texture analyzer (Stable Micro Systems Ltd., Surrey, UK).

#### 2.6.3. WHC

The WHC of the MP gels was tested according to the method of Li et al. (2019) with slight modifications. Each treatment was repeated at least three times. WHC (%) was calculated as follows:

$$\text{WHC}\,(\%) = \frac{m_2 - m_0}{m_1 - m_0} \times 100 \quad (1)$$

where $m_0$ represents the mass of the centrifuge tube, $m_1$ represents the combined weight of the MP gels and centrifuge tube, and $m_2$ represents the mass after centrifugation at 3,000 rpm, 4 °C for 10 min.

#### 2.6.4. Whiteness of gel

The whiteness of the gel was determined using a CR-400 colorimeter (Konica Minolta Holdings, Inc., Tokyo, Japan) to measure $L^*$ (brightness), $a^*$ (redness), and $b^*$ (yellowness). This instrument was equipped with a D65 illuminant, a 2° observer with an 8 mm aperture measuring area. The whiteness value was then calculated by the following formula:

$$\text{Whiteness} = 100 - \sqrt{(100 - L^*)^2 + a^{*2} + b^{*2}}$$

#### 2.6.5. Low-field nuclear magnetic resonance (LF-NMR)

Headspace vials (2 mL) with blue threaded plastic caps containing 1.65 g of gel (final protein concentration of 30 mg/mL) were placed into cylindrical glass tubes with a diameter of 15 mm and measured using an LF-NMR analyzer (NMI20, Niumag Analytical Instrument Co. Ltd., Suzhou, China). The sample relaxation time ($T_2$) values were determined using the Carr − Purcell − Meiboom − Gill sequence.

#### 2.6.6. Microstructure

Gel samples of MPs (4 × 4 × 4 $mm^3$) were pretreated with glutaraldehyde and a gradient series of ethanol solutions (Ma et al., 2022). The dried gel samples were gold-plated prior to imaging. Subsequently, the microstructure of the gel was observed using a Sigma 300 scanning electron microscope (Zeiss AG, Oberkochen, Germany) at 10,000 × magnification.

### 2.7. Statistical analysis

Data were collected from three independent experiments conducted on different days and expressed as mean ± standard error (SE). The data were analyzed by ANOVA using Statistix 9.0 (Analytical Software, Tallahassee, FL, USA), followed by Tukey's multiple range test for comparison of the means ($P < 0.05$). Figures were created using SigmaPlot 12.5 software and Origin 2023.

## 3. Results and discussion

### 3.1. Amino acid group changes

#### 3.1.1. Carbonyls

The carbonyl group increase is considered the most important chemical change in protein oxidation and is thus the best indicator for the quantitative analysis of oxidation reactions, a higher carbonyl content in proteins indicates more oxidative damage to proteins (Estévez, 2011). As shown in Fig. 1a, the carbonyl content of the MPs sample oxidized by •OH (O) was 1.46 nmol/mg, which was 1.83 times that of the No-O sample (0.80 nmol/mg) ($P < 0.05$). However, the carbonyl content significantly decreased as the EG concentration increased ($P < 0.05$), showing a maximum decrease of 60.0 % in the presence of $EG_H$ (50 mg/g). This result correlates with the gradual increase in hydroxyl groups with increasing EG concentration, which further promotes its cross-linking with proteins. This reflects the ability of polyphenols to effectively inhibit protein carbonylation reactions and scavenge •OH, preventing the generation of carbonyl groups and protecting proteins from free radical attack. Cao, True, Chen, and Xiong (2016) found that the presence of gallic acid also significantly inhibited the carbonyl formation, especially at high doses, reducing the carbonyl content by up to 55.4 % compared with oxidized MPs.

#### 3.1.2. Total sulfhydryls

The change in total sulfhydryl content is commonly measured to assess the extent of protein oxidation. MPs are abundant in sulfhydryl groups, particularly for the myosin, which contains approximately 40 sulfhydryl groups per myosin molecule. As shown in Fig. 1b, oxidation decreased the sulfhydryl content of MPs by 5.93 %, from 75.08 nmol/mg before oxidation (No-O) to 70.63 nmol/mg after the oxidation treatment (O). Sulfhydryl groups are readily oxidized by •OH into intramolecular or intermolecular disulfide (-SS-) bonds, directly affecting the structure of the protein and its functions and properties (Xiong, Park, & Ooizumi, 2009). Adding EG to the MPs under oxidized conditions reduced the total sulfhydryl content compared to the No-O sample, probably because of the cross-linking reaction between EG and MPs. The hydroxyl groups in the molecular structure of phenolic compounds are easily converted to quinones by oxidation. Quinones react with sulfhydryl groups in protein molecules to form sulfhydryl − quinone adducts by the Michael addition reaction, effectively decreasing the sulfhydryl content in protein molecules. In this context, Jongberg, Lund, Waterhouse, and Skibsted (2011) attributed the increased loss of sulfhydryl groups when 4-methylcatechol was injected into beef proteins under oxidizing conditions to the nucleophilic (Michael) addition reaction, which ultimately protected the protein oxidation sites and prevented the formation of -SS-

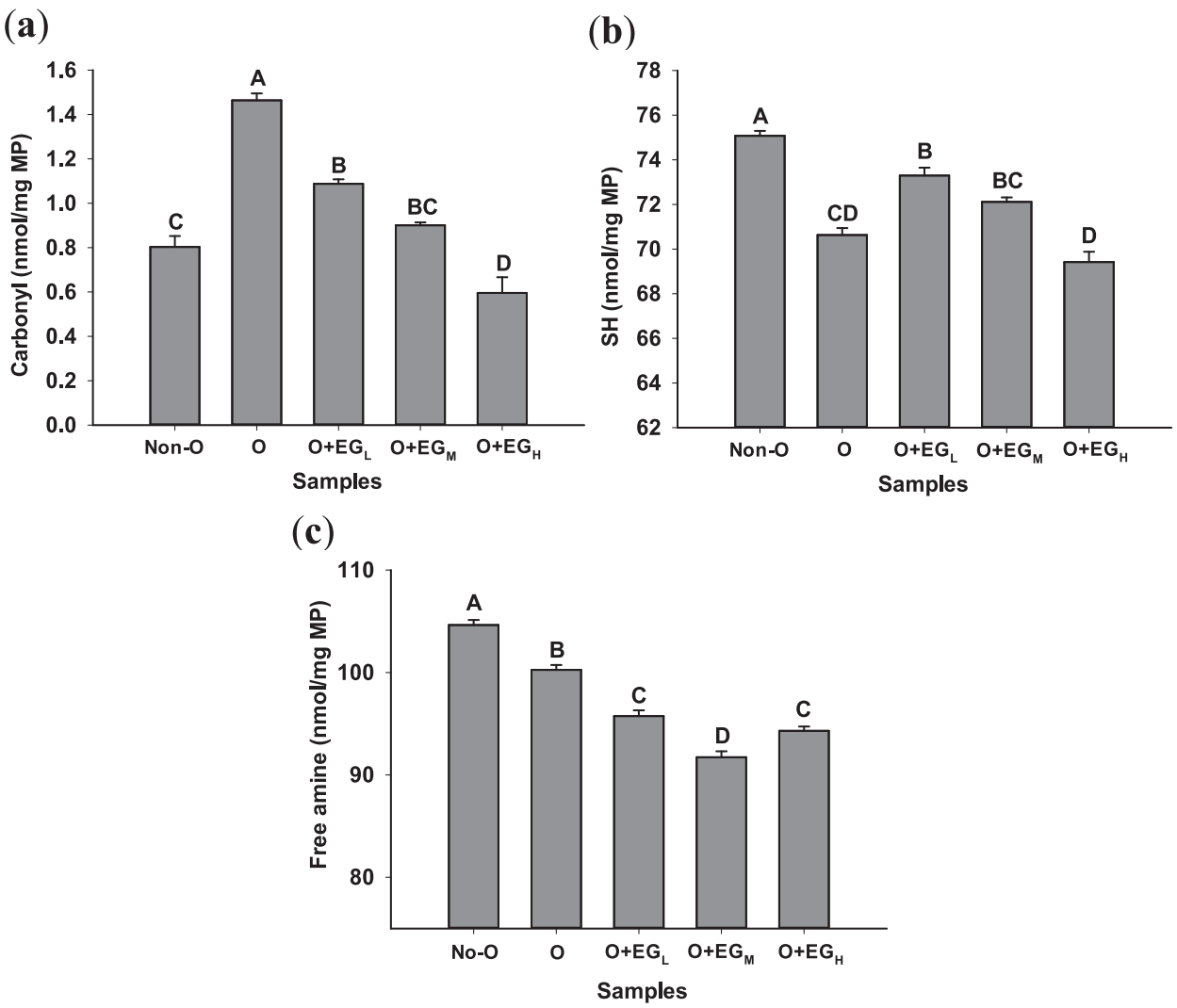


**Fig. 1.** Carbonyl content (a), total sulfhydryl (SH) content (b), and free amine content (c) of myofibrillar protein (MP) treated with various amounts of eugenol (EG) under oxidizing conditions. No-O, non-oxidized; O, oxidized; O + $EG_L$, O + $EG_M$, and O + $EG_H$, oxidized in the presence of EG at 5, 20, and 50 mg/g protein, respectively. Mean (±SE) values followed by different superscript letters (A − D) in the same parameter group indicate significant differences ($P < 0.05$).

bonds through protein − protein oxidation reactions. Compared to the oxidized control (O), the total sulfhydryl content increased by 2.66 and 1.49 nmol/mg when $EG_L$ (5 mg/g) and $EG_M$ (20 mg/g) were added, respectively, and was further accelerated by $EG_H$. This concentration-dependent effect of EG on the total sulfhydryl groups of MPs is mainly due to two reasons: on the one hand, phenolics enhance the contact between sulfhydryl groups by changing the electrostatic force, thereby increasing the chance of reactions between sulfhydryl groups and promoting the formation of -SS- bonds (Cao & Xiong, 2015). On the other hand, it is possible that the addition of EG caused the unfolding of the MPs molecules and led to the exposure of buried sulfhydryl groups to •OH during the early stage of the reaction.

### 3.1.3. Free amines

The content of free amino groups is typically used to reflect the degree of oxidation of the ε-$NH_2$ group of lysine (Cao & Xiong, 2015). As shown in Fig. 1c, compared to No-O, approximately 4.18 % of the free amine content was lost when the MPs sample was exposed to the •OH-generating system (O). The addition of EG did not significantly prevent the loss of free amino groups. On the contrary, it tended to promote -SH and ε-$NH_2$ oxidation, especially the $EG_M$ treatment (20 mg/g), which showed an approximate 8.52 % loss, indicating that the presence of EG could not effectively prevent the oxidation-induced decrease in the free amino content. It is widely known that readily available lysine residues can be deaminated, forming Schiff-base adducts with carbon-based derivatives under oxidative conditions (Levine, Garland, Oliver, et al. 1990). On the one hand, the loss of free amino groups could arise from the covalent cross-links by the Schiff-base reaction between amino groups and semiquinones or quinones, on the other hand, could be attributed to the measurement of free amino acids with a 1 % SDS solution, which destroyed the non-covalent interactions. Therefore, a covalent interaction between phenolic compounds and MPs may contribute to the loss of free amino groups. Supporting this view, a related study reported that mulberry polyphenols contributed to the loss of free amino groups from MPs by the covalent addition of free amino groups to quinones (Cheng, Zhu, & Liu, 2020).

## 3.2. Changes in protein structure

### 3.2.1. Secondary structure

The exact position of the amide I band and the corresponding secondary structures of EG-modified MPs under oxidative stress were quantified by FTIR spectroscopy. In the second-derivative spectra, the main peaks of protein secondary structures are observed in the amide I band spectral region (1600–1700 $cm^{-1}$), including the β-sheet (1600–1640 $cm^{-1}$), random coil (1641–1650 $cm^{-1}$), α-helix

(1651–1660 $cm^{-1}$), and β-turn (1661–1700 $cm^{-1}$).

As shown in Fig. 2a − 2e, there were nine visible peaks for each sample, indicating the complex secondary structure of MPs. The No-O sample displayed peaks at 1613.4, 1613.4, 1624.1, 1634.5, 1645.0, 1655.5, 1666.4, 1677.9, and 1689.3 $cm^{-1}$, which were similar to those reported by Zhao, Zhang, Li, et al. (2018), who identified nine characteristic absorption bands in the infrared spectral region for the secondary structures of proteins and peptides. Of particular note was the wave number representing the α-helix structure in the protein, which shifted from 1655.5 $cm^{-1}$ for No-O to 1658.3 $cm^{-1}$ for oxidized sample. This result indicates that oxidation led to an increase in the electron cloud density of C═O and a reduction in hydrogen bonding forces and was consistent with the carbonyl content results. A similar phenomenon was found by Ma, Pan, Dong, et al. (2022) when they studied the secondary structure of porcine MPs oxidized by clove extract. However, the oxidation-induced shift to a larger wave number was somewhat inhibited by adding the three different concentrations of EG to the MPs under oxidative stress (1658.0, 1656.4, and 1656.4 $cm^{-1}$), suggesting that EG inhibits the deterioration of the MPs secondary structure.

Fig. 2f shows the effect of varying the concentration of EG on the secondary structures of MPs, expressed as percentages. After oxidation by •OH, the α-helix, β-turn, and random coil were reduced, and the β-sheet content was increased compared to the No-O control. After α-helix deconvolution, part of the peptide chain was converted into a folded structure. This rearrangement led to a decrease in the structural and conformational stability of the protein, thus exposing the hydrophobic residues buried initially inside the molecule, which further enhanced the hydrophobic interactions between myosin molecules and contributed to protein aggregation and increased hydrophobicity of the protein surface (Wu, Zhang, & Hua, 2009), which is consistent with the section 3.2.3 above results for $H_o$. It was also shown in Fig. 2f that the β-sheet content of EG-modified MPs was less than that of oxidized samples and significantly higher than that of No-O, again indicating that the general oxidation mode of MPs was altered by the addition of EG. The slight increase in β-sheet in O + $EG_L$ compared to oxidized sample is probably attributable to the fact that $EG_L$ protected amino acids, such as proline and glycine, as well as the β-sheet against free radical attack (Zhao, et al., 2019). The α-helix content of the MP samples added with $EG_H$ was higher than that of the oxidized MP samples but lower than that of the No-O sample. In summary, the addition of EG can, to some extent, restrain the displacement of the amide I band. It is noteworthy that the addition of $EG_H$ could effectively protect the secondary structure of the protein against •O-induced structural changes of MPs and reduce the degree of oxidative protein polymerization.

### 3.2.2. Intrinsic tryptophan fluorescence

In order to examine the effect of various concentrations of EG on the conformational changes in oxidized MPs, intrinsic tryptophan fluorescence was used. As illustrated in Fig. 3a, compared to the No-O control, the intrinsic tryptophan fluorescence intensity of MPs decreased ($P < 0.05$) after exposure to •OH, and a fluorescence quenching occurred, which is consistent with the observations of Gan, Li, Wang, et al. (2019) and Li et al. (2019) concerning the reduction in fluorescence intensity after oxidative treatment of MPs. It was also noticed that compared to the oxidized sample, the addition of EG remarkedly prevented the attenuation of fluorescence intensity, and the intrinsic tryptophan fluorescence intensity gradually raised with the increase of EG concentration from 5 to 50 mg/g. In particular, the O + $EG_H$ sample progressively approached the No-O sample, presumably owing to the high concentration of EG offsetting the fluorescence quenching caused by oxidation, and the maximum emission wavelength was blue-shifted from 320 nm (No-O) to 315 nm (O + $EG_H$). This result was probably attributed to the protein-protective effect of $EG_H$ during free radical attack due to its strong antioxidant activity.

### 3.2.3. $H_o$ analysis

The degree of binding of hydrophobic amino acids in protein with BPB was used to express the $H_o$. From the results (Fig. 3b), the amount of BPB bound to the oxidized sample was significantly increased by 1.76 times to 5.52 μg compared to the No-O sample, suggesting that oxidation triggers the unfolding of the protein structure, revealing more hydrophobic amino acid residues on the protein surface. There was no significant ($P > 0.05$) change in the amount of BPB between the O + $EG_L$ and O + $EG_M$, but the amount of BPB was remarkably less than in the oxidized sample. By contrast, the BPB binding of O + $EG_H$ (50 mg/g) was higher than that of the oxidized sample. Benjakul, Visessanguan, Ishizaki, and Tanaka (2001) found that a moderate increase in $H_o$ can promote hydrophobic interactions in thermally induced gels; moreover, an increase in $H_o$ indicates the unfolding of the protein structure (Cheng, Zhu, & Liu, 2020). Therefore, more reactive groups can participate in the gel formation process, promoting covalent or non-covalent protein − protein and protein − EG cross-linking, thus facilitating the formation of gel network structures, which is consistent with the results of gel strength (discussed later in section 3.4.2). A similar investigation found that adding mulberry polyphenol (0.5 %) to MPs also increased the $H_o$ and confirmed that appropriate concentrations of mulberry polyphenols could increase the $G'$ value of MP gels (Huang, Sun, Liu, et al., 2022). Jia Sun Liu Jin & Liu (2021) reported that a high addition of quercetin (150 μmol/g) slightly increased the $H_o$ of MPs, thus promoting hydrophobic interactions between proteins during thermally induced gel formation.

## 3.3. Protein cross-linking

SDS-PAGE was carried out to assess the cross-linking behavior of MP samples in response to oxidation and EG treatment. As presented in Fig. 3c, in the absence of βME, compared to the No-O control sample, oxidation significantly accelerated protein cross-linking as demonstrated by the loss of both the myosin heavy chain (MHC) and tropomyosin (Tm) bands, indicating that oxidation caused aggregation of macromolecules, with more polymers appearing at the top of the stacking gel. However, compared to the oxidation sample, the addition of EG remarkedly increased the intensity of both the MHC and Tm bands to that similar to the No-O sample, indicating the protein-protective ability of EG. Accompanying this was the observation of cross-linked bands above the MHC after the addition of EG compared to the By contrast, the BPB binding of O + $EG_H$ (50 mg/g) was higher than that of the By contrast, the BPB binding of O + $EG_H$ (50 mg/g) was higher than that of the oxidized sample and No-O control samples, possibly because excess EG can induce cross-linking of proteins, which may occur internally within the molecule and not be as damaging as oxidation-induced cross-linking.

The presence of βME (+βME) mostly all of the MHC bands, Actin bands, and Tm were recovered, mainly -SS- polymerization occurred, indicating that this aggregation was reducible. The addition of EG induced the polymerization of MPs, and these protein polymers were mainly formed by -SS- bonds, which is a typical covalent cross-linking in MPs. Combined with the decrease in sulfhydryl content discussed in section 3.1.2, it can be concluded that some sulfhydryl groups may have formed -SS- bonds. nevertheless, under reducing conditions, βME chemically reduced the -SS- of the samples and allowed separation of individual peptide chains. In any case, $EG_H$ finally enhanced the band intensity of MHC and Tm.

## 3.4. Gelling properties

### 3.4.1. Dynamic rheological changes

The changes in $G'$ of the MPs suspension during the heating process are illustrated in Fig. 4. $G'$ reflects the elastic changes of the gel, which should be analyzed considering springiness (Huang, Sun, Liu, et al., 2022). The No-O sample displayed a typical $G'$ curve, with two transition peaks at approximately 50 and 62 °C, respectively. An initial elastic gel

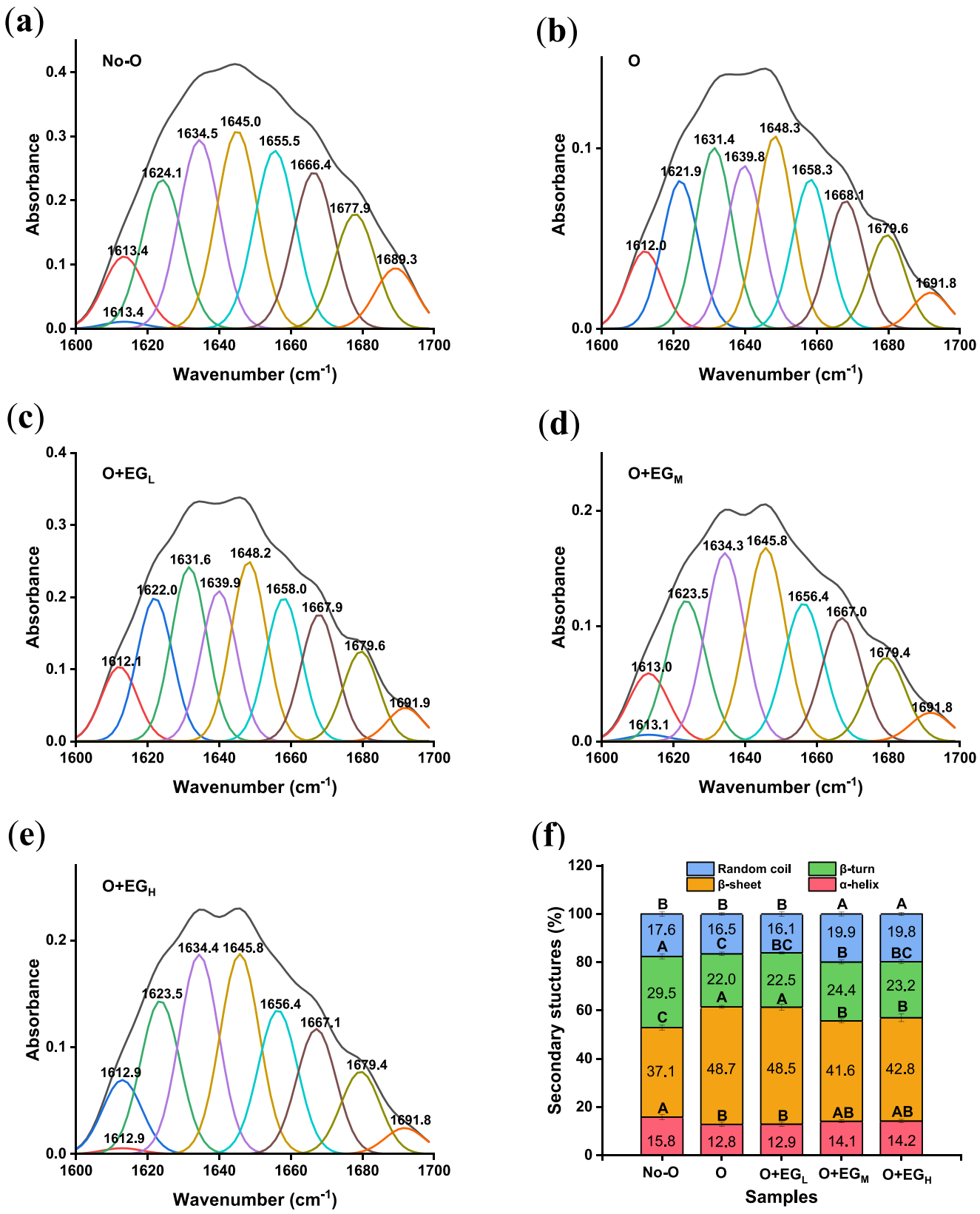


**Fig. 2.** Fourier-transform infrared spectroscopy amide I band profiles (a − e) and secondary structure (f) of myofibrillar protein (MP) treated with various amounts of eugenol (EG) under oxidizing conditions. No-O, non-oxidized; O, oxidized; O + $EG_L$, O + $EG_M$, and O + $EG_H$, oxidized in the presence of EG at 5, 20, and 50 mg/g protein, respectively. Mean (±SE) values followed by different superscript letters (A − C) in the same parameter group indicate significant differences ($P < 0.05$).

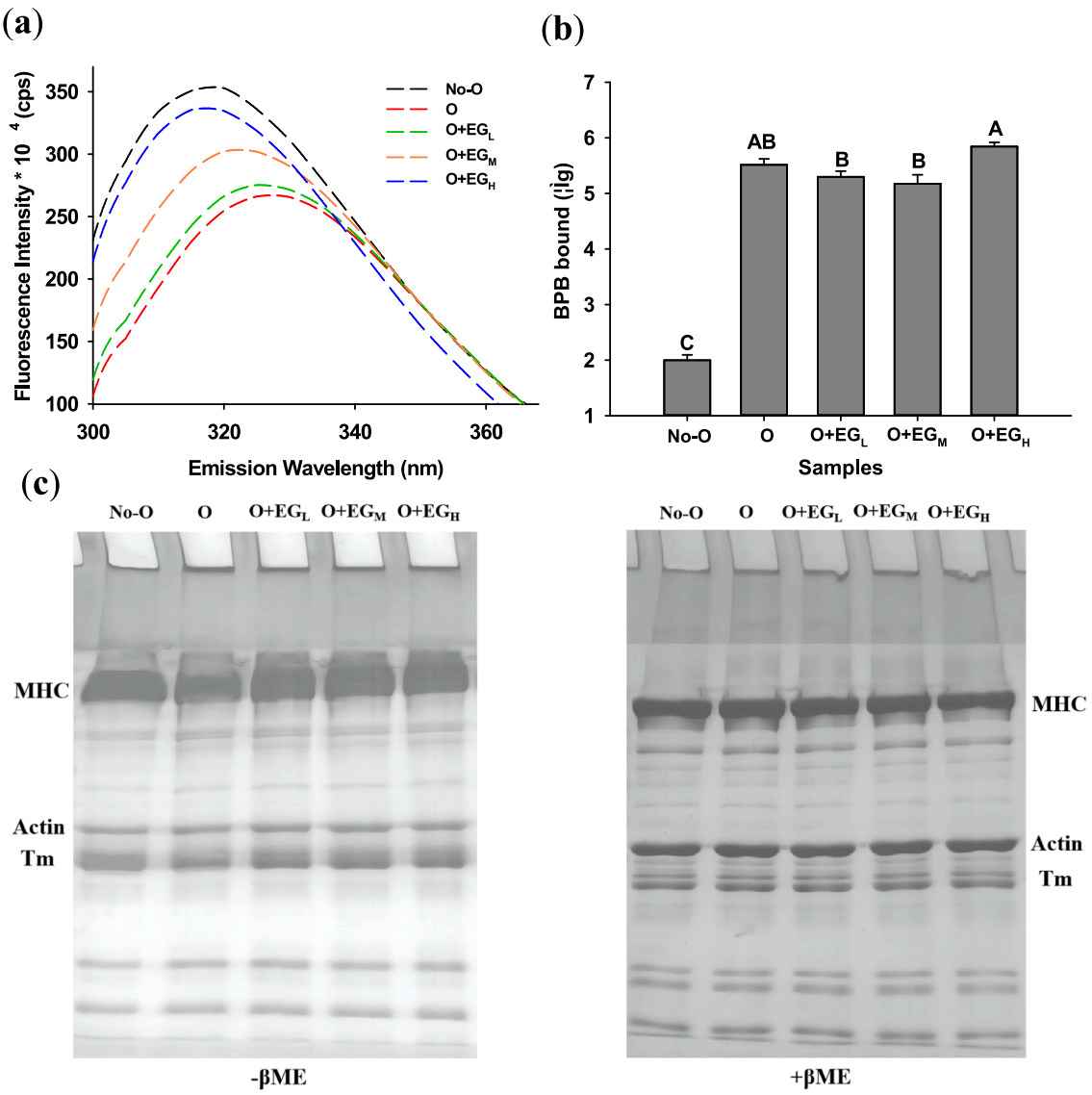


**Fig. 3.** Intrinsic tryptophan fluorescence (a), surface hydrophobicity (BPB fluorescence) (b), and SDS–PAGE patterns (c) of myofibrillar protein (MP) treated with various amounts of eugenol (EG) under oxidizing conditions. No-O, non-oxidized; O, oxidized; O + $EG_L$, O + $EG_M$, and O + $EG_H$, oxidized in the presence of EG at 5, 20, and 50 mg/g protein, respectively. Mean (±SE) values followed by different superscript letters (A – C) in the same parameter group indicate significant differences ($P < 0.05$).

is formed between 35 and 50 °C, primarily due to the head-to-head association of uncoiled myosin molecules. The $G'$ values then decrease from 50 to 62 °C, leading to tail – tail aggregation of myosin and destruction of the network structure, resulting in weaker gel elasticity (Li, Kang, Xiang, et al., 2020). Finally, the protein unfolds due to thermal denaturation and displays a continuous increase in $G'$ due to the intense myosin head – head interactions and tail – tail interactions when the temperature approximately exceeds 62 °C, forming an irreversible and typical MP gels network (Huang, Sun, Liu, et al., 2022).

As shown in Fig. 4, although the rheological curves of O + $EG_L$ and oxidized sample were comparable, the final $G'$ of O + $EG_L$ was significantly higher than that of oxidized sample. When the temperature was 50 °C (the first peak), the $G'$ of O + $EG_M$ and O + $EG_H$ were 102 and 105 Pa, respectively, which were 57.87 % (O + $EG_M$) and 37.19 % (O + $EG_H$) lower than the oxidized sample (243 Pa). This may be because some of the EG molecules play an antioxidant role, while the remaining EG may be detrimental to the unfolding of MPs and inhibit the involvement of more reactive groups in gel formation by interfering with head-to-head cross-linking or reducing the number of exposed hydrophobic groups (Fig. 3b). When the temperature was 62 °C (the second peak), the peak temperature was 59 °C (O), 58 °C (O + $EG_L$), 51 °C (O + $EG_M$), and 51 °C (O + $EG_H$), indicating that the tail-to-tail cross-linking was affected and had an appreciable influence on the final protein network structure. However, when the temperature was 72 °C, the final $G'$ of the MPs added with EG groups (O + $EG_L$: 521 Pa, O + $EG_M$: 422 Pa, O + $EG_H$: 648 Pa) was significantly higher than that of the oxidized sample (353 Pa). Jia Sun Liu Jin & Liu (2021) also found that the addition of quercetin significantly enhanced the final $G'$ of MPs in an oxidative system.

### 3.4.2. *Changes in gel strength and whiteness*

Gel strength is one of the parameters that reflect the gel properties and edibility of meat products. As shown in Fig. 5a, the gel strength of the oxidized gel was significantly ($P < 0.05$) reduced by 25.48 % compared to the No-O gel. This indicates that oxidation destroys the protein structure, resulting in a reduced ability of the protein to form gels. Compared to the oxidized sample, all three concentrations of EG significantly increased the gel strength by 16.35 % (O + $EG_L$), 9.62 % (O + $EG_M$), and 21.08 % (O + $EG_H$), respectively ($P < 0.05$). Besides the

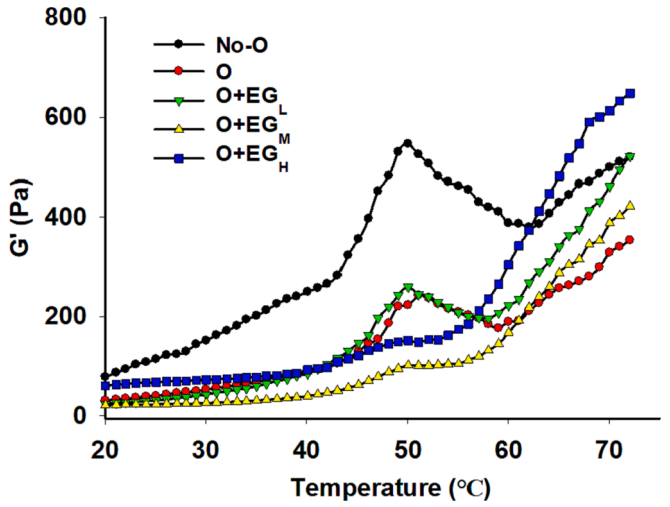


**Fig. 4.** Storage modulus ($G'$) of myofibrillar protein (MP) treated with various amounts of eugenol (EG) under oxidizing conditions. No-O, non-oxidized; O, oxidized; O + $EG_L$, O + $EG_M$, and O + $EG_H$, oxidized in the presence of EG at 5, 20, and 50 mg/g protein, respectively.

antioxidant effects, this may be because the addition of EG leads to an increase in the hydrophobicity of the protein surface due to the unfolding of the protein structure, which contributes to the formation of the gel structure. Cao, True, Chen, and Xiong (2016) also found that the structure of MPs gels could be improved by hydrogen bonding and hydrophobic interactions induced by phenolic compounds, including (−)-epigallocatechin-3-gallate. In addition, Nie, Zhao, Wang, and Meng (2017) found that the conversion of sulfhydryl groups in MPs into disulfide bonds during thermally induced gel formation was one of the main forces maintaining the gel. The results of the sulfhydryl group analysis showed that the addition of EG increased the sulfhydryl content, probably due to the increased -SS- cross-linking between the proteins as a result of the phenol − protein interaction, which facilitated gel formation. Therefore, the addition of EG has a positive effect on the strength of the protein gel.

Gel whiteness can reflect the color and quality characteristics of MP gels (Chen et al., 2023). As shown in Fig. 5b, the oxidation treatment increased the whiteness value of the MP gels compared to the No-O gel. The whiteness values were slightly higher for O + $EG_L$ (75.86) and O + $EG_M$ (76.61) compared to the oxidized sample (75.60), but the difference was not significant ($P > 0.05$). This suggests that EG does not affect the whiteness of the gels when the EG functions as an antioxidant. For O + $EG_H$ (50 mg/g), the whiteness values increased significantly to 78.84 ($P < 0.05$) compared to the oxidized sample (75.60). Therefore, an appropriate concentration of EG effectively enhanced the whiteness of MP gels.

### 3.4.3. WHC change in gel

WHC provides a quantitative indication of the amount of water maintained within the protein gel structure, and this could reflect aspects of the spatial structure of the gel. As shown in Fig. 5c, the WHC of the gel formed by the oxidized sample was significantly lower than that of the No-O control sample, indicating that the oxidative damage in myosin could result in an inferior gel network formation, causing lower elasticity and poor WHC in the gel matrix. When EG was added, the WHC values increased significantly ($P < 0.05$) from 52.33 % (O) to 57.03 % (O + $EG_L$), 58.29 % (O + $EG_M$) and 69.80 % (O + $EG_H$). In particular, when $EG_H$ was added, the water retention of the gels reached a maximum of 69.80 %, indicating that EG has a strong free radical scavenging capacity, which can effectively prolong the oxidation process, protect the protein side chain structure, and enhance the cross-linking ability of the protein, thus forming a stronger network structure with better water retention capacity. These same efforts were reported by Li et al. (2019) for tea polyphenols on MPs under oxidative conditions, who also found a concentration-dependent improvement in the WHC of the gels.

### 3.4.4. LF-NMR change of gels

The LF-NMR technique is efficient in assessing water distribution and mobility during protein gel formation. The $T_2$ relaxation time reflects the degree of water freedom in the gel; $T_2$ increases as the water interaction with macromolecules decreases and water mobility improves (Wang et al., 2021). As shown in Fig. 5d, three peaks were observed and directly assigned to three distinct water classes, including $T_{20}$ (10–100 ms), $T_{21}$ (100–1,000 ms), and $T_{22}$ (1,000–10,000 ms), which represent the bound water in macromolecular structures, immobilized water trapped within the gel network structures, and free water, respectively.

As shown in Table 1, compared to the No-O control gel, oxidation significantly reduced the proportion of immobilized water ($P_{21}$) and remarkably increased the proportion of free water ($P_{22}$) in the MP gels ($P < 0.05$). This suggests that protein oxidation resulted in the conversion of immobilized water into free water, which explains the significant decrease in WHC observed in the MP gels due to oxidation (Fig. 5c). Ma, Yuan, Feng, et al. (2022) also found similar results, showing that oxidation significantly decreased the area ratio of immobile water and increased the area ratio of free water in the MP gels. The addition of EG significantly suppressed the oxidation-induced transformation of bound water and immobilized water in the MP gels to free water. The $P_{21}$ for the three EG groups significantly increased from 74.96 % (O) to 81.72 % (O + $EG_L$), 82.28 % (O + $EG_M$), and 94.46 % (O + $EG_H$) ($P < 0.05$). However, $P_{22}$ decreased from 23.92 % in the gel formed from oxidized sample to 17.25 % (O + $EG_L$), 16.72 % (O + $EG_M$), and 4.34 % (O + $EG_H$). Moreover, $EG_H$ caused a significant ($P < 0.05$) increase in $T_{21}$, from 132.19 ms (O) to 151.99 ms (O + $EG_H$) (Table 1), whereas $T_{22}$ was significantly lower than that for O + $EG_L$ and O + $EG_M$ ($P < 0.05$), indicating restricted mobility of free water. Therefore, more water was retained in the gel networks, resulting in an increase in WHC.

### 3.5. Microstructure of gels

The microstructure of MP gels formed from Non-O and oxidized sample. MPs with and without EG were observed by scanning electron microscopy, as shown in Fig. 5e. The MPs in the No-O control exhibited a tightly bound state and homogeneous microstructure with tiny pores. In comparison, the gel formed from oxidized MPs exhibited numerous large pores, heterogeneous and irregular clumps, as well as hills and gullies. This phenomenon was caused by the oxidation-induced cross-linking and protein aggregation in the MPs emulsion, and these gaps may promote water channel formation and negatively affect muscle WHC. Although the network structure of MPs added with EG was not as orderly and homogeneous as that of the No-O control sample, it was found that the introduction of EG reduced the empty spaces and transformed the loose and heterogeneous gel structure of gel formed from the oxidized sample into a dense and smooth network, The best performance was observed for O + $EG_H$, which exhibited a fine, uniform, and compact microstructure. This result indicated that the phenolic compounds and proteins were more tightly bound to each other by hydrogen bonding and hydrophobic interactions. These findings were consistent with the analysis of gel strength (Fig. 5a), WHC (Fig. 5c), and water distribution (Fig. 5d), demonstrating that adding $EG_H$ can effectively improve the gel quality of the oxidized MPs (O), which can successfully delay oxidation-induced damage to muscle tissue structure. Similar results have been reported by Ma, Yuan, Feng, et al. (2022), who found that the introduction of ε-polylysine (ε-PL) ameliorated the microstructure of oxidized MP gels, especially when ε-PL was added at 0.020 %, resulting in a fine, uniform, and compact microstructure.

Based on the experimental analysis results, we propose a hypothetical mechanism for the effects of O + $EG_H$ on myosin gelling properties

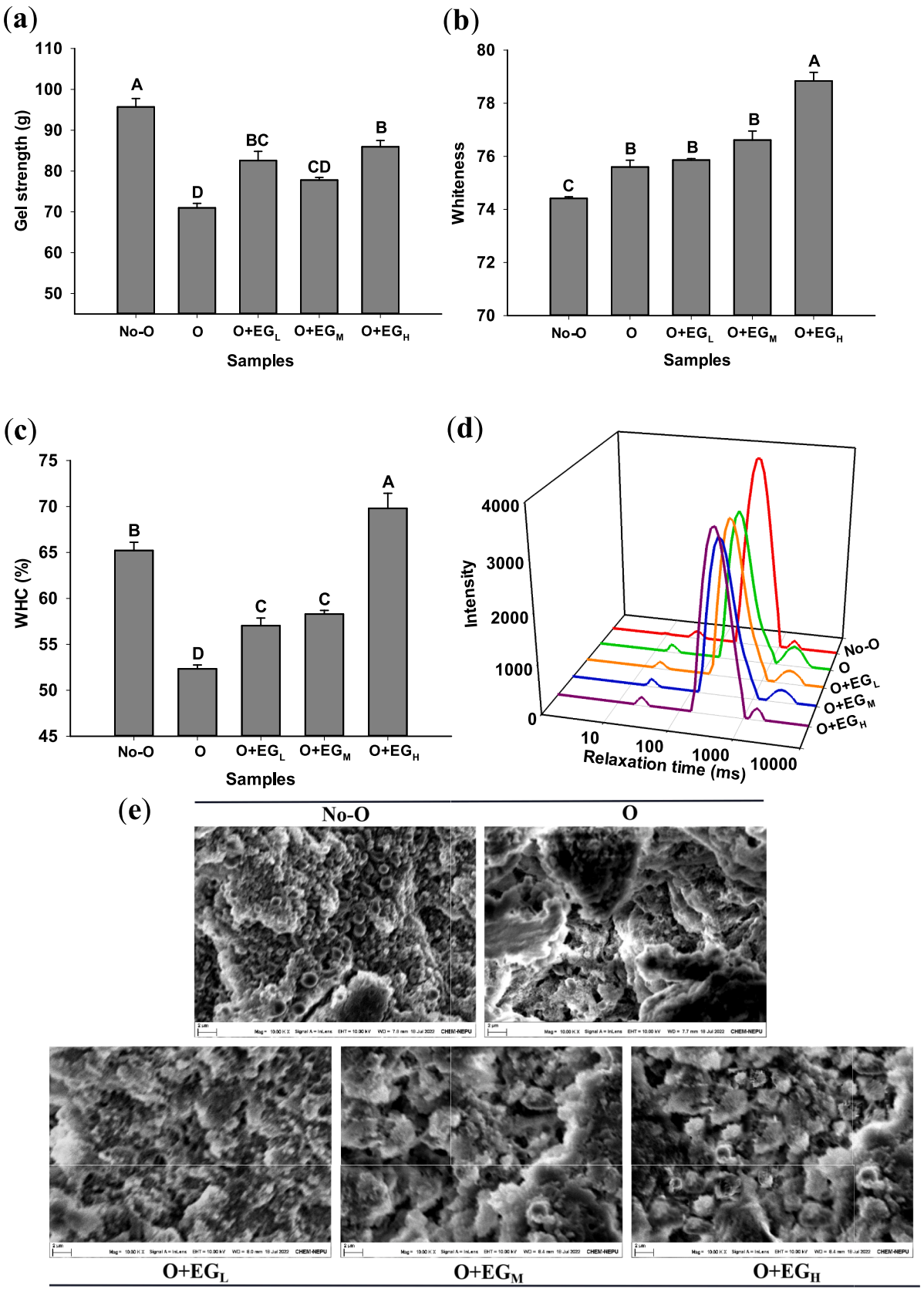


**Fig. 5.** Gel strength (a), whiteness (b), water-holding capacity (WHC) (c), curve of $T_2$ relaxation time (d), and scanning electron micrographs (e) of myofibrillar protein (MP) treated with various amounts of eugenol (EG) under oxidizing conditions. No-O, non-oxidized; O, oxidized; O + $EG_L$, O + $EG_M$, and O + $EG_H$, oxidized in the presence of EG at 5, 20, and 50 mg/g protein, respectively. Mean (±SE) values followed by different superscript letters (A − D) in the same parameter group indicate significant differences ($P < 0.05$).

**Table 1**
Changes in relaxation times and proportion of peak areas of myofibrillar protein (MP) gels treated with different concentrations of eugenol (EG).

| Sample | $T_{20}$ (ms) | $T_{21}$ (ms) | $T_{22}$ (ms) | $P_{20}$ (%) | $P_{21}$ (%) | $P_{22}$ (%) |
|---|---|---|---|---|---|---|
| No-O | 24.77 ± 0.42$^{A}$ | 174.75 ± 8.69$^{A}$ | 1417.45 ± 41.23$^{B}$ | 1.48 ± 0.02$^{A}$ | 96.71 ± 2.69$^{A}$ | 1.81 ± 0.19$^{D}$ |
| O | 14.17 ± 0.24$^{D}$ | 132.19 ± 6.11$^{C}$ | 1232.85 ± 38.77$^{C}$ | 1.12 ± 0.10$^{BC}$ | 74.96 ± 1.10$^{C}$ | 23.92 ± 0.44$^{A}$ |
| O + $EG_L$ | 14.17 ± 0.26$^{D}$ | 132.19 ± 6.84$^{C}$ | 1629.75 ± 56.68$^{A}$ | 1.02 ± 0.07$^{C}$ | 81.72 ± 1.39$^{B}$ | 17.25 ± 0.51$^{B}$ |
| O + $EG_M$ | 16.30 ± 0.33$^{C}$ | 132.19 ± 6.36$^{C}$ | 1629.75 ± 53.55$^{A}$ | 1.00 ± 0.05$^{C}$ | 82.28 ± 2.12$^{B}$ | 16.72 ± 0.80$^{B}$ |
| O + $EG_H$ | 18.74 ± 0.21$^{B}$ | 151.99 ± 5.36$^{B}$ | 1232.85 ± 41.05$^{C}$ | 1.21 ± 0.04$^{B}$ | 94.46 ± 2.32$^{A}$ | 4.34 ± 0.56$^{C}$ |

Values are given as mean ± SE from triplicate determinations.
Means followed by superscripts with different letters (A – D) in the same column are significantly different ($P < 0.05$).
[#]No-O, non-oxidized; O, oxidized; O + $EG_L$, O + $EG_M$, and O + $EG_H$ oxidized in the presence of EG at 5, 20, and 50 mg/g protein, respectively.

under oxidation conditions. As shown in Fig. 6, during the heating process of myosin, the No-O samples could form an ordered three-dimensional gel network structure by virtue of head-to-head and tail-to-tail cross-linking. On the contrary, oxidation causes denaturation of myosin, which is dominated by tail-to-tail cross-linking and results in a loose network-like structure with large gaps in the gel (Xiong, Blanchard, Ooizumi, et al., 2010). However, for O + $EG_H$, much better elastic gels were formed after heating, probably because heat-induced cross-linking of myosin was influenced by the large amount of EG, suggesting that not only can EG exert antioxidant properties but also that excess EG can induce cross-linking of proteins, which may occur internally within the molecule and not be as damaging as oxidation-induced cross-linking, thereby improving head-to-head and tail-to-tail cross-linking. Moreover, the rheological and gel strength results revealed that O + $EG_H$ increased the final $G'$ and gel strength compared to the No-O sample, despite forming a gel network structure almost the same as that of the No-O sample.

## 4. Conclusions

Treatment with $EG_L$, $EG_M$, and $EG_H$ significantly enhanced the WHC and gelling properties of oxidatively stressed MPs, mainly by regulating the protein conformation and modulating the gelation behavior. The most effective EG concentration was $EG_H$, indicating that the well-maintained fluorescence intensity, secondary structure, and $H_o$, reduced carbonyl content and free amines content, and improved viscoelastic properties. This may be because some of the EG molecules counteract the oxidation, while others interact with the MPs and increase the final $G'$ during gelation, resulting in a fine and compact three-dimensional network structure that could reduce the mobility of the water. The results in this paper are helpful in understanding the effect of EG in meat systems under oxidation conditions and provide a way to improve the functional characteristics of oxidative meat proteins.

## CRediT authorship contribution statement

**Deyin Pan:** Formal analysis, Data curation, Writing – original draft. **Jinming Ma:** Writing – review & editing, Methodology, Software. **Jingjing Diao:** Investigation, Validation, Conceptualization. **Jiaqi Li:** Data curation. **Hongsheng Chen:** Project administration, Funding

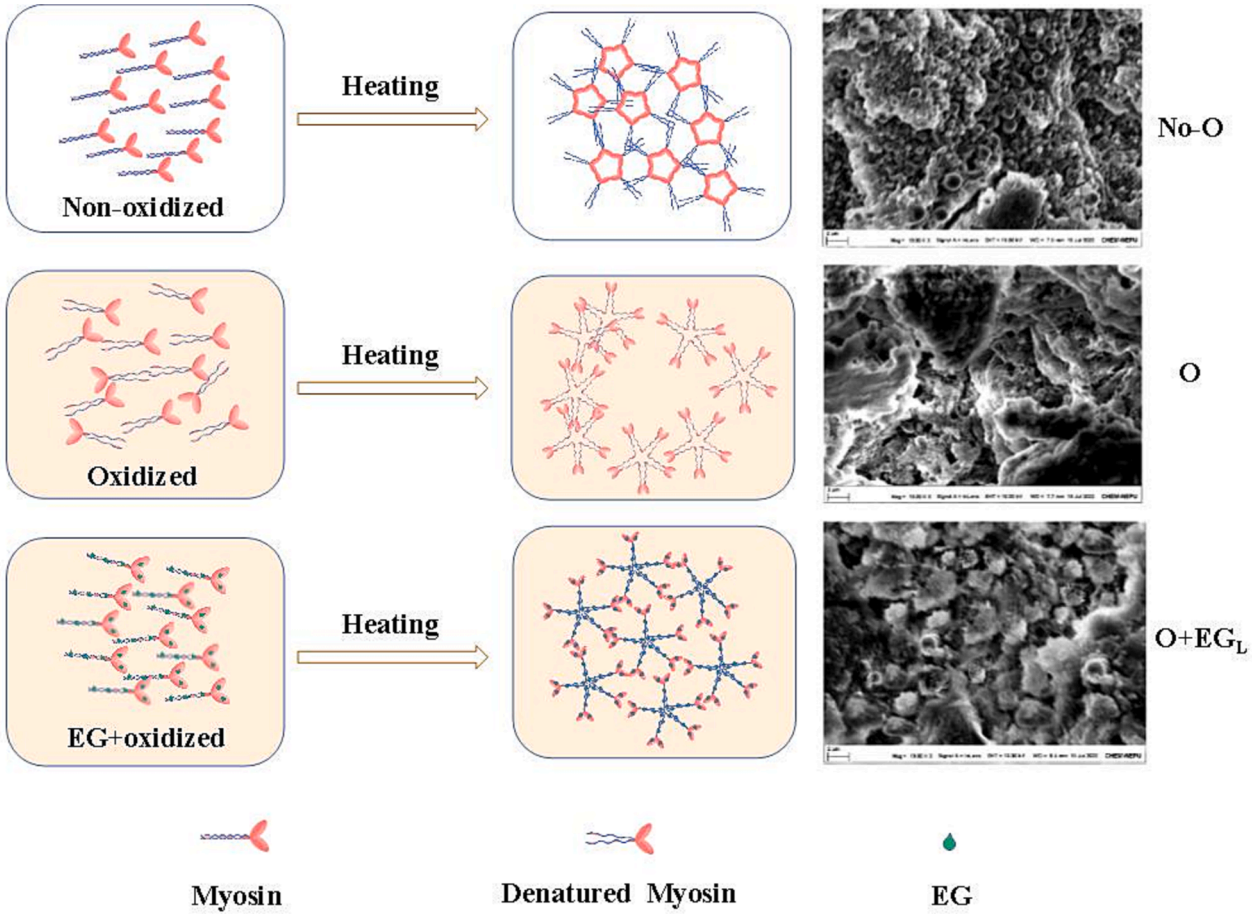


**Fig. 6.** Schematic of the interaction mechanism between myofibrillar protein (MP) and eugenol (EG) under oxidation conditions.

acquisition, Supervision.

## Declaration of Competing Interest

The authors declare that they have no known competing financial interests or personal relationships that could have appeared to influence the work reported in this paper.

## Data availability

Data will be made available on request.

## Acknowledgments

Funding: This research was supported by the Major Science and Technology Projects, Heilongjiang Province, China [grant number 2020ZX07B02] and the "Three Horizontal and Three Vertical" Support Program Project of Heilongjiang Bayi Agricultural University [grant numberTDJH202003].

## References

Benjakul, S., Visessanguan, W., Ishizaki, S., & Tanaka, M. (2001). Differences in gelation characteristics of natural actomyosin from two species of bigeye snapper, priacanthus tayenus and priacanthus macracanthus. *Journal of Food Science, 66*(9), 1311–1318. https://doi.org/10.1111/j.1365-2621.2001.tb15207.x

Cao, Y., Ma, W., Huang, J., & Xiong, Y. (2020). Effects of sodium pyrophosphate coupled with catechin on the oxidative stability and gelling properties of myofibrillar protein. *Food Hydrocolloids, 104*, Article 105722. https://doi.org/10.1016/j.foodhyd.2020.105722

Cao, Y., True, A., Chen, J., & Xiong, Y. (2016). Dual role (anti-and pro-oxidant) of gallic acid in mediating myofibrillar protein gelation and gel in vitro digestion. *Journal of Agricultural and Food Chemistry, 64*(15), 3054–3061. https://doi.org/10.1021/acs.jafc.6b00314

Cao, Y., & Xiong, Y. (2015). Chlorogenic acid-mediated gel formation of oxidatively stressed myofibrillar protein. *Food Chemistry, 180*, 235–243. https://doi.org/10.1016/j.foodchem.2015.02.036

Chen, H., Diao, J., Li, Y., Chen, Q., & Kong, B. (2016). The effectiveness of clove extracts in the inhibition of hydroxyl radical oxidation-induced structural and rheological changes in porcine myofibrillar protein. *Meat Science, 111*, 60–66. https://doi.org/10.1016/j.meatsci.2015.08.017

Chen, H., Ma, J., Pan, D., Diao, J., Guo, A., Li, R., & Xiong, Y. L. (2023). Concentration-dependent effect of eugenol on porcine myofibrillar protein gel formation. *Meat Science, 201*, Article 109187. https://doi.org/10.1016/j.meatsci.2023.109187

Chen, X., Chen, K., Cheng, H., & Liang, L. (2022). Soluble aggregates of myofibrillar proteins engineered by gallic acid: Colloidal structure and resistance to in vitro gastric digestion. *Journal of Agricultural and Food Chemistry, 70*(13), 4066–4075. https://doi.org/10.1021/acs.jafc.1c05840

Cheng, J., Zhu, M., & Liu, X. (2020). Insight into the conformational and functional properties of myofibrillar protein modified by mulberry polyphenols. *Food Chemistry, 308*, Article 125592. https://doi.org/10.1016/j.foodchem.2019.125592

El-Maati, M., Mahgoub, S., Labib, S., Al-Gaby, A., & Ramadan, M. (2016). Phenolic extracts of clove (syzygium aromaticum) with novel antioxidant and antibacterial activities. *European Journal of Integrative Medicine, 8*(4), 494–504. https://doi.org/10.1016/j.eujim.2016.02.006

Estévez, M. (2011). Protein carbonyls in meat systems: A review. *Meat Science, 89*(3), 259–279. https://doi.org/10.1016/j.meatsci.2011.04.025

Estévez, M., & Heinonen, M. (2010). Effect of phenolic compounds on the formation of α-aminoadipic and γ-glutamic semialdehydes from myofibrillar proteins oxidized by copper, iron, and myoglobin. *Journal of Agricultural and Food Chemistry, 58*(7), 4448–4455. https://doi.org/10.1021/jf903757h

Gan, X., Li, H., Wang, Z., Emara, A., Zhang, D., & He, Z. (2019). Does protein oxidation affect proteolysis in low sodium Chinese traditional bacon processing? *Meat Science, 150*, 14–22. https://doi.org/10.1016/j.meatsci.2018.10.007

Geng, F., Huang, Y., Huang, Q., He, D., Li, S., & Ma, M. (2018). Effect of hydroxyl radical-induced oxidation on the structure and heat-induced gel properties of ovalbumin. *Journal of Food Processing and Preservation, 42*(6). https://doi.org/10.1111/jfpp.13626

Gürbüz, M., & Korkmaz, B. (2022). The anti-campylobacter activity of eugenol and its potential for poultry meat safety: A review. *Food Chemistry, 394*, Article 133519. https://doi.org/10.1016/j.foodchem.2022.133519

Huang, X., Sun, L., Liu, L., Wang, G., Luo, P., Tang, D., & Huang, Q. (2022). Study on the mechanism of mulberry polyphenols inhibiting oxidation of beef myofibrillar protein. *Food Chemistry, 372*, Article 131241. https://doi.org/10.1016/j.foodchem.2021.131241

Jia, N., Sun, J., Liu, D., Jin, B., & Liu, D. (2021). Effect of quercetin on the structure and gel properties of pork myofibrillar protein under oxidative conditions. *Food Science, 42*(10), 45–51. https://doi.org/10.7506/spkx1002-6630-20191103-021

Jiang, J., & Xiong, Y. (2016). Natural antioxidants as food and feed additives to promote health benefits and quality of meat products: A review. *Meat Science, 120*, 107–117. https://doi.org/10.1016/j.meatsci.2016.04.005

Jongberg, S., Lund, M., Waterhouse, A., & Skibsted, L. (2011). 4-methylcatechol inhibits protein oxidation in meat but not disulfide formation. *Journal of Agricultural and Food Chemistry, 59*(18), 10329–10335. https://doi.org/10.1021/jf202268q

Levine, R., Garland, D., Oliver, C., Amici, A., Climent, I., Lenz, A., … Stadtman, E. (1990). Determination of carbonyl content in oxidatively modified proteins. *Methods in Enzymology, 186*, 464–478. https://doi.org/10.1016/0076-6879(90)86141-H

Li, K., Kang, C., Xiang, Q., Zhao, D., & Bai, Y. (2020). Effect of atmospheric pressure plasma jet on structural and rheological properties of chicken myofibrillar protein. *Food Science, 41*(19), 124–131. https://doi.org/10.7506/spkx1002-6630-20190916-202

Li, L., Ji, H., Kang, D., Zhou, Y., & Guo, Y. (2019). Effect of tea polyphenols on physicochemical and gel properties of pork myofibrillar protein under oxidative conditions. *Food Science, 40*(2), 12–17. https://doi.org/10.7506/spkx1002-6630-20180606-064

Lin, L., Mei, C., Shi, C., Li, C., Abdel-Samie, M., & Cui, H. (2023). Preparation and characterization of gelatin active packaging film loaded with eugenol nanoparticles and its application in chicken preservation. *Food Bioscience, 53*, Article 102778. https://doi.org/10.1016/j.fbio.2023.102778

Ma, J., Pan, D., Dong, Y., Diao, J., & Chen, H. (2022). The effectiveness of clove extract on oxidization-induced changes of structure and gelation in porcine myofibrillar protein. *Foods, 11*(13), 1970. https://doi.org/10.3390/foods11131970

Ma, W., Yuan, F., Feng, L., Wang, J., Sun, Y., Cao, Y., & Huang, J. (2022). E-polylysine-mediated enhancement of the structural stability and gelling properties of myofibrillar protein under oxidative stress. *International Journal of Biological Macromolecules, 220*, 1114–1123. https://doi.org/10.1016/j.ijbiomac.2022.08.143

Marchese, A., Barbieri, R., Coppo, E., Orhan, I., Daglia, M., Nabavi, S., … Ajami, M. (2017). Antimicrobial activity of eugenol and essential oils containing Eugenol: A mechanistic viewpoint. *Critical Reviews in Microbiology, 43*(6), 668–689. https://doi.org/10.1080/1040841X.2017.1295225

Nie, X., Zhao, L., Wang, N., & Meng, X. (2017). Phenolics-protein interaction involved in silver carp myofibrillar protein films with hydrolysable and condensed tannins. *LWT-food Science and Technology, 81*, 258–264. https://doi.org/10.1016/j.lwt.2017.04.011

Park, D., Xiong, Y., & Alderton, A. (2007). Concentration effects of hydroxyl radical oxidizing systems on biochemical properties of porcine muscle myofibrillar protein. *Food Chemistry, 101*(3), 1239–1246. https://doi.org/10.1016/j.foodchem.2006.03.028

Purkait, S., Bhattacharya, A., Bag, A., & Chattopadhyay, R. (2020). Evaluation of antibiofilm efficacy of essential oil components β-caryophyllene, cinnamaldehyde and eugenol alone and in combination against biofilm formation and preformed biofilms of listeria monocytogenes and salmonella typhimurium. *Letters in Applied Microbiology, 71*(2), 195–202. https://doi.org/10.1111/LAM.13308

Rajkovic, A., Tomasevic, I., Meulenaer, B. D., & Devlieghere, F. (2017). The effect of pulsed UV light on escherichia coli O157: H7, listeria monocytogenes, salmonella typhimurium, staphylococcus aureus and staphylococcal enterotoxin a on sliced fermented salami and its chemical quality. *Food Control, 73*, 829–837. https://doi.org/10.1080/1040841X.2017.1295225

Souza, K. D., Monteschio, J. D. O., Mottin, C., Ramos, T., Pinto, L. D. M., Eiras, C., … Prado, I. D. (2019). Effects of diet supplementation with clove and rosemary essential oils and protected oils (eugenol, thymol and vanillin) on animal performance, carcass characteristics, digestibility, and ingestive behavior activities for nellore heifers finished in feedlot. *Livestock Science, 220*, 190–195. https://doi.org/10.1016/j.livsci.2018.12.026

Taguri, T., Tanaka, T., & Kouno, I. (2004). Antimicrobial activity of 10 different plant polyphenols against bacteria causing food-borne disease. *Biological and Pharmaceutical Bulletin, 27*(12), 1965–1969. https://doi.org/10.1248/bpb.27.1965

Tan, P., Ye, T., Liu, X., & He, J. (2010). Research advances in antioxidant composition of botanical extracts and their action mechanisms. *Food Science, 31*, 288–292.

Torrecilhas, J., Ornaghi, M., Passetti, R., Mottin, C., Guerrero, A., Ramos, T., … Prado, I. D. (2021). Meat quality of young bulls finished in a feedlot and supplemented with clove or cinnamon essential oils. *Meat Science, 174*, Article 108412. https://doi.org/10.1016/j.meatsci.2020.108412

Wang, L., Wang, X., Ma, J., Yang, K., Feng, X., You, X., … Wang, L. (2021). Effects of radio frequency heating on water distribution and structural properties of grass carp myofibrillar protein gel. *Food Chemistry, 343*, Article 128557. https://doi.org/10.1016/j.foodchem.2020.128557

Wu, W., Zhang, C., & Hua, Y. (2009). Structural modification of soy protein by the lipid peroxidation product malondialdehyde. *Journal of the Science of Food and Agriculture, 89*(8), 1416–1423. https://doi.org/10.1002/jsfa.3606

Xiong, Y., Blanchard, S., Ooizumi, T., & Ma, Y. (2010). Hydroxyl radical and ferryl-generating systems promote gel network formation of myofibrillar protein. *Journal of Food Science, 75*(2), 215–221. https://doi.org/10.1111/j.1750-3841.2009.01511.x

Xiong, Y., Park, D., & Ooizumi, T. (2009). Variation in the cross-linking pattern of porcine myofibrillar protein exposed to three oxidative environments. *Journal of Agricultural and Food Chemistry, 57*(1), 153–159. https://doi.org/10.1021/jf8024453

Yilmaz, M., Hassanein, W., Alkabaa, A., & Ceylan, Z. (2022). Electrospun eugenol-loaded gelatin nanofibers as bioactive packaging materials to preserve quality characteristics of beef. *Food Packaging and Shelf Life, 34*, Article 100968. https://doi.org/10.1016/j.fpsl.2022.100968

Zhao, B., Zhang, S., Li, S., Zhou, H., Ren, S., Li, J., … Wang, S. (2018). Effect of lipid oxidation on myofibrillar protein oxidation, structure and functional characteristics. *Food Science, 39*(5), 40–46. https://doi.org/10.7506/spkx1002-6630-201805007

Zhao, X., Zhou, Y., Zhao, L., Chen, L., He, Y., & Yang, H. (2019). Vacuum impregnation of fish gelatin combined with grape seed extract inhibits protein oxidation and degradation of chilled tilapia fillets. *Food Chemistry, 294*, 316–325. https://doi.org/10.1016/j.foodchem.2019.05.054

Zheng, Y., Zhou, F., Zhang, L., Wang, H., & Wang, X. (2021). Effect of different extent of protein oxidation on the frozen storage stability of muscle protein in obscure pufferfish (Takifugu obscurus). *LWT-Food Science and Technology, 137*, Article 110416. https://doi.org/10.1016/j.lwt.2020.110416